BMC Gastroenterology

RESEARCH Open Access

M64HCl, a focal adhesion kinase activator, promotes intestinal mucosal healing in rats

Guiming Liu[1*], Ahmed Adham R. Elsayed[1], Louis Boafo Kwantwi[1], Ricardo Gallardo-Macias[2], Vadim J. Gurvich[2] and Marc D. Basson[1*]

Abstract

Background Intestinal mucosal injury may arise from various factors. While many drugs target the causative factors, none directly stimulate mucosal wound healing. We found that the specific focal adhesion kinase (FAK) activator, M64HCl, promotes intestinal mucosal healing in mice. This study aims to further validate the therapeutic impact of M64HCl on intestinal mucosal repair in rats as a second species.

Methods Wistar rats were assigned to one of four groups: normal control, 1-day injury + vehicle, 4-day injury + vehicle, or 4-day injury + M64HCl. Intestinal injury was induced by serosally applying 75% acetic acid. Immediately after injury, rats received either a continuous infusion of M64HCl (25 mg/kg/day) or its vehicle (saline). Four days post-injury, blood was drawn to measure M64HCl levels and assess liver and kidney function. The intestines were removed and opened, ulcer areas were photographed for size quantification, and tissues were fixed for histological and immunohistochemical analysis.

Results M64HCl substantially reduced ulcer area on gross examination, while histological analysis showed alleviation of pathological changes with M64HCl treatment. Immunohistochemical analysis confirmed increased immunoreactivity for phosphorylated FAK in the epithelium adjacent to the injury in M64HCl-treated rats. However, there was no change in the percentage of Ki67-positive cells in each crypt at the edge of the ulcer area. Serum creatinine, ALT, and AST levels did not differ between the 4-day injury groups with or without M64HCl treatment.

Conclusions M64HCl, a water-soluble FAK activator, promotes acetic acid-induced ulcer healing in rats and may be useful in treating gastrointestinal mucosal injury.

Keywords Focal adhesion kinase, Small intestine, mucosal injury, Mucosal healing

*Correspondence:
Guiming Liu
gliu@neomed.edu
Marc D. Basson
mbasson@neomed.edu
[1]Department of Biomedical Sciences, Northeast Ohio Medical University College of Medicine, 4209 State Route 44, Rootstown, OH, USA
[2]Institute for Therapeutics Discovery and Development, Department of Medicinal Chemistry, College of Pharmacy, University of Minnesota, Minneapolis, MN, USA

Introduction

The mucosa is the innermost layer of the gastrointestinal tract, consisting of the epithelium, lamina propria, and muscularis mucosae. The intestinal epithelium, the largest mucosal surface in the body, spans approximately 400 m^2 in humans and is comprised of a single cell layer organized into villi and crypts. The epithelial cells lining the intestinal surface include enterocytes, goblet cells, enterochromaffin cells, M-cells, and Paneth cells [1]. Various pathogenic factors, such as alcohol, ischemia-reperfusion injury, stress, radiation, medications like nonsteroidal anti-inflammatory drugs (NSAIDs), and chemotherapy can cause damage to the intestinal mucosa. For instance, up to 70% of individuals consuming NSAIDs show small bowel mucosal injury (including erosions, ulceration, and mucosal hemorrhage) when undergoing video capsule endoscopy [2]. This type of injury can result in occult small bowel bleeding, and NSAID use is suspected to be the cause in 10–15% of patients with iron deficiency anemia [3]. Currently, acid-suppressive drugs, such as proton pump inhibitors (PPIs), and/or mucoprotective agents like eupatilin, are commonly used to prevent gastrointestinal (GI) bleeding [4]. However, the protective effects of PPIs are limited to the upper GI tract and do not extend beyond the duodenum. In fact, PPIs may even cause injury to the lower GI tract [5].

Focal Adhesion Kinase (FAK), a 125 kDa non-receptor protein tyrosine kinase, is a crucial component of integrin signaling [6]. FAK plays a pivotal role in regulating focal adhesion dynamics and is involved in various cellular processes such as cell adhesion, survival, and migration [7]. Activated FAK is critically involved in intestinal epithelial wound healing, [8] but activated FAK levels are actually decreased adjacent to mucosal injury because of decreased FAK synthesis [9, 10, 11]. We therefore postulated that FAK activators could be used to treat mucosal injuries. While searching the ZINC (recursive acronym: ZINC is not commercial) database for small molecules that mimic a key subdomain of the N-terminal FERM (four-point-one, ezrin, radixin, moesin) domain of FAK, we discovered that ZINC40099027 could dose-dependently activate FAK phosphorylation, stimulate wound closure in the human epithelial cell line Caco-2 monolayer, and promote mucosal healing in murine small bowel ulcers induced by topical serosal acetic acid application or subcutaneous indomethacin injection [12]. However, ZINC40099027 is not water-soluble, necessitating dimethyl sulfoxide (DMSO) solubilization. Recently, we synthesized and evaluated a third-generation water-soluble compound, M64HCl, designed through structure-activity relationship studies. This compound exhibits promising drug-like properties. M64HCl activates FAK, promotes epithelial sheet migration in vitro, and accelerates intestinal mucosal wound healing in mice [13]. However, drugs frequently work differently in different species. The current study therefore aimed to verify the therapeutic efficacy of M64HCl in treating intestinal injuries induced by topical serosal acetic acid in rats. We sought to test the hypothesis that rats treated with M64HCl after ulcerogenesis would exhibit small ulcer areas than rats exposed to a similar ulcerogenic process receiving vehicle alone.

Materials and methods

Experimental reagents

1-(2-(dimethylamino)-2-(pyridin-4-yl)ethyl)-3-(2-morpholino-5-(trifluoromethyl)phenyl) urea hydrochloric salt (M64HCl) was synthesized at the Institute for Therapeutics Discovery and Development and Department of Medicinal Chemistry, College of Pharmacy, University of Minnesota. The molecular formula is: $C_{21}H_{27}ClF_3N_5O_2$, and the molecular weight is 473.9. The structure, synthesis, and quality control were described in detail in our previous publication [13]. The purity of the synthesized M64HCl was 95.8%. Horiba ALT (SGPT) and AST (SGOT) reagents were bought from HORIBA Medical (Irvine, CA, USA). Creatinine assay kit (#6041) was from Chondrex Inc (Woodinville, WA, USA). Glacial acetic acid (#A38S-500) was from Fisher Chemical (Fair Lawn Industrial Park, NJ, USA). Rabbit anti-phospho-FAK (Tyr397) (BS-3159R) was purchased from Bioss Inc (Woburn, MA). Ki67 (D3B5) Rabbit mAb (#34330) was bought from Cell Signaling (Danvers, MA).

Experimental animals, intestine injury induction, and M64HCl treatment

Male (268–310 g) and female (175–222 g) Wistar rats aged 10 to 11 weeks old (Charles River Laboratory, Wilmington, MA) were used in this study. Rats were housed in an animal facility with controlled conditions: temperature at 22 °C, humidity at 50% ± 5%, and a 12-hour light/dark cycle using artificial lighting. They had free access to tap water and commercial chow. After a one-week acclimatization period, the rats were assigned to one of the following four groups: **(1)** Normal control group ($n = 4$), **(2)** 1-day injury + vehicle group ($n = 6$), **(3)** 4-day injury + vehicle group ($n = 6$), or **(4)** 4-day injury + M64HCl group ($n = 6$).

Okabe et al. [14] introduced an acetic acid-induced gastric mucosal injury model. Ulcers in this model are reproducibly induced and heal spontaneously. We previously made slight modifications to induce and characterize the mucosal injury in the intestine and have extensively published this model in both mice [12, 13, 15, 16, 17] and rats [18]. Simply, after anesthesia with 1.5–2.5% isoflurane, an ischemic ulcer was induced by placing circular filter disks (3.14 mm^2) saturated with 75% acetic acid directly on

the antimesenteric serosa of the small intestine, approximately 8 cm proximal to the cecum, for 30 s, without opening the bowel. Animals were then randomly allocated to receive either a continuous infusion of M64HCl (25 mg/kg/day) or a saline vehicle using osmotic pumps (model1007D, Alzet, Cupertino, CA) for four consecutive days as described previously [13]. Meanwhile, the normal control animals received nothing. The osmotic pumps were surgically implanted subcutaneously immediately after inducing the injury in the small intestine. Briefly, an ALZET osmotic pump was filled with either the vehicle (saline) or M64HCl solution. A small incision was made slightly posterior to the scapulae. A hemostat was used to create a pocket, and the filled pump was inserted into the pocket with the cap flush inside. The incision was closed with wound clips.

Four days after injury induction and/or treatment, blood was collected via cardiac puncture under 2% isoflurane anesthesia to measure M64HCl levels and biochemical parameters. Subsequently, the animals were euthanized by inhalation of 3–4% isoflurane until respiratory arrest, followed by thoracotomy as a secondary method. The intestines were rapidly removed, and the ulcers, along with the adjacent non-ulcerated areas, were photographed to measure ulcer areas using ImageJ software (NIH). Intestinal tissues were also harvested from the normal control animals as well as from a group of rats one day after ulcerogenesis. The tissues were then fixed in 10% neutral-buffered formalin for histological and immunohistochemical examination. All experimental procedures were approved by the Institutional Animal Care and Use Committee (IACUC) of Northeast Ohio Medical University, with IACUC number 23-04-366.

Histology

Rat small intestine tissues were fixed for 48 h, then processed and embedded in paraffin. Five-micron sections were cut and stained with hematoxylin and eosin. Histopathological changes observed in the H&E-stained sections were scored in three categories: inflammatory cell infiltration, hemorrhage, and epithelial disruption. A scale of 0 to 5 was used to represent different levels (0 indicates none, while 5 represents extensive), based on previous publications [19]. All images were assessed by two independent observers who were blinded to the group assignments, and the mean values were used for statistical analysis.

Immunohistochemistry

Five-micron sections were used for immunohistochemical staining, following our previously established method [13]. In brief, the sections underwent dewaxing and rehydration using graded ethanol. Subsequently, heat-induced epitope retrieval was performed with citrate buffer, followed by treatment with 0.3% hydrogen peroxide in methanol to neutralize endogenous peroxidase. The sections were then incubated with blocking buffer at room temperature for 30 min, followed by overnight incubation at 4 °C with primary antibodies [rabbit FAK (Tyr397) polyclonal antibody, BS-3159R, Bioss Inc., Woburn, MA, or Ki67 (D3B5) Rabbit mAb, #34330, Cell Signaling, Danvers, MA]. After three 5-minute rinses, the sections were exposed to secondary antibodies (biotinylated goat anti-rabbit IgG, Vector, Burlingame, CA) for 2 h at room temperature. Subsequently, the Avidin-Biotin Complex (ABC) staining method was employed. Finally, the sections were counterstained with hematoxylin.

Sections undergoing the same procedures, but without the primary antibody, were used to confirm the specificity of immunoreactive staining. The intensity of p-FAK immunoreactivity in the migrating epithelium at the ulcer edge was assessed as previously described, [13] with a score of 0 indicating minimal detectable staining and 4 representing the highest staining intensity. All images were evaluated by two independent observers who were blinded to the group assignments, and the mean values were used for statistical analysis. Cellular proliferation in intestinal crypts was evaluated using Ki67 immunolabeling. All epithelial cells within each crypt were counted, and the percentage of Ki67-positive cells was calculated.

Ultra-performance liquid chromatography-mass spectrometry (UPLC-MS) measurement of serum M64HCl levels

M64HCl was measured as previously described [13]. Twenty microliters of serum were mixed with methanol to reach a final concentration of 80%. After centrifugation at 2000 g for 10 min, the precipitated proteins were separated, and 10 µl of the resulting supernatant was injected into the UPLC-MS/MS system for analysis. Separation on the UPLC system was conducted using a Waters Acquit I Class UPLC system with a Waters ACQUITY UPLC HSS T3 column (1.8 µM, 100 Å pore diameter, 2.1 × 150 mm) and an ACQUITY UPLC HSS T3 precolumn (1.8 µM, 100 Å pore diameter, 2.1 × 5 mm), maintained at 55 °C. A linear gradient of solvents A (0.1% formic acid in water) and B (0.1% formic acid in acetonitrile) was employed at a flow rate of 0.3 mL/min. The initial percentage of solvent B was increased from 1 to 25% within the first minute of separation, followed by a further increase to 90% over 1.9 min, reaching equilibrium at 5 min with solvent B returning to 1%, allowing for a 4-minute equilibration period between injections.

MS/MS analysis was conducted using the Waters Xevo TQ-S triple quadrupole mass spectrometer (Waters, Milford, MA) in multiple reaction monitoring mode. The mass spectrometer operated in a positive electrospray ionization (ESI) mode. For quantification, the following

mass transitions were employed: 438.2/273.1 (CE 25), while for analyte confirmation, transitions 438.2/192.1 (CE 20) and 438.2/149.2 (CE 24) were utilized. MassLynx V4.1 controlled the UPLC-MS/MS system, and quantification was carried out against an M64HCl external standard using a generated response curve.

Assays for liver and kidney function markers

The blood samples collected were transferred into red BD vacutainer serum tubes (367820, BD, Franklin Lakes, NJ). Allow the samples to clot at room temperature for 45–60 min, then centrifuge the samples at 1,500 g for 15 min. The resulting supernatants were then frozen at -80 °C for later measurement of serum ALT and AST activities (Horiba Medical, Irvine, CA), as well as creatinine levels (#6041, Chondrex Inc, Woodinville, WA), using commercial kits and following the manufacturer's instructions.

Statistical analysis

Statistical analysis was conducted using GraphPad Prism 6 (GraphPad Software, La Jolla, CA). Data are expressed as mean ± standard deviation (SD). The ulcer areas in one sample from the 4-day injury + vehicle group and one sample from the 4-day injury + M64HCl group were not captured in sectioning and were excluded from the quantification. Comparisons for ulcer area, histopathological scoring, p-FAK immunoreactivity and Ki67 immunoreactive positive cells, as well as serum ALT, AST and creatinine were made between the 4-day injury + vehicle and 4-day injury + M64HCl groups using an unpaired 2-tailed t-test to test our primary hypothesis. *P*-values less than 0.05 were considered statistically significant.

Results

M64HCl promotes intestinal mucosal healing in rats

Gross observations revealed well-demarcated ulcer craters in the injury groups. Representative images of acetic acid-induced intestinal ulcers in a vehicle-treated rat at day 1 (**A**), day 4 (**B**), and an M64HCl-treated rat at day 4 (**C**) are shown in Fig. 1. ImageJ software was used to measure the digital images of intestinal ulcers by manually tracing their contours. Quantification data (Fig. 1D) showed the largest ulcer area one day after injury induction. The ulcer area was substantially smaller in the 4-day injury + M64HCl group compared to the 4-day injury + vehicle group ($p = 0.0474$). This indicates that M64HCl administration accelerates the healing of acetic acid-induced intestinal ulcers in rats. The serum concentration of M64HCl in treated rats at the time of euthanasia was 344.5 ± 218.6 ng/mL, corresponding to 726.8 ± 461.3 nM.

Histological examination

Figure 2A shows the normal histology of the rat small intestine, characterized by slender, uniform villi, crypts, a submucosa and muscle layers. The ulcer crater was visible in the 1-day injury + vehicle group (Fig. 2B), the 4-day injury + vehicle group (Fig. 2C) and the injury + M64HCl group (Fig. 2D), although it was more pronounced in the injury + vehicle groups. Compared to the normal histological structure of the intestine, which features intact intestinal villi and crypts of Lieberkühn, the ulcerated area exhibited hemorrhage, disruption of the mucosa, submucosa, and even the muscular layer. Inflammatory cells were observed infiltrating the area to varying extents. Histopathological scoring demonstrated that these pathological changes were significantly alleviated in the 4-day injury + M64HCl group compared to the 4-day injury + vehicle group ($p = 0.0057$, Fig. 2E).

Expression of p-FAK and Ki67 in the adjacent area of ulcers

Immunohistochemistry was used to compare p-FAK immunoreactivity among different groups. The immunoreactive intensity of p-FAK in the adjacent mucosal area of the 1-day injury + vehicle rats (Fig. 3B) was comparable to that of the control rats (Fig. 3A). In the 4-day injury + vehicle rats (Fig. 3C), p-FAK immunoreactive cells were primarily located in the crypts, with notably weak expression in the epithelium at the edge of the ulcer area. Conversely, stronger p-FAK staining was observed in both the intestinal crypts and villi of injured animals treated with M64HCl (Fig. 3D), suggesting enhanced FAK activation (Fig. 3E). Ki67-positive cells were primarily located in the crypts across all groups, and the percentage of Ki67-positive cells per small intestinal crypt remained consistent among the groups (Fig. 4).

M64HCl infusion does not affect rat hepatic and renal function

Serum levels of alanine aminotransferase (ALT), aspartate aminotransferase (AST), and creatinine were measured to assess hepatic and renal function in the 4-day injury + M64HCl group and the 4-day injury + vehicle group. No significant differences were observed in serum ALT, AST, or creatinine levels between the two groups (Table 1), indicating that M64HCl administration at 25 mg/kg/day did not affect hepatic or renal function.

Discussion

The intestinal epithelial barrier acts as the first line of defense against the harsh environment of the intestinal lumen [20]. Following injury, the intestinal mucosa undergoes a healing process to restore its barrier function. This process involves a complex interaction among various cell types, cytokines, mediators, and the vascular system [21]. Immune cells such as macrophages,

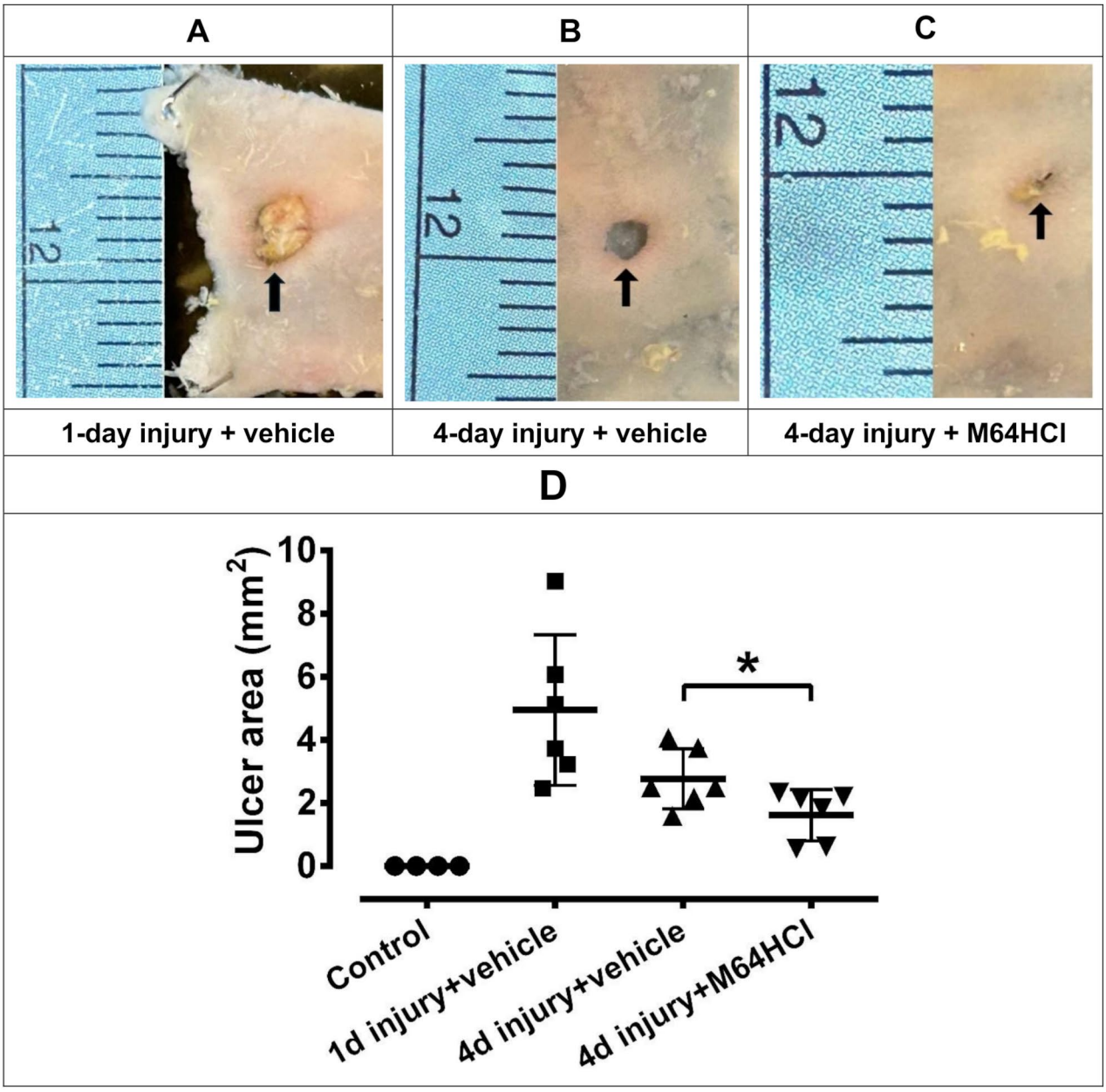

Fig. 1 Administration of M64HCl accelerates the healing of acetic acid-induced intestinal ulcers in rats. Representative images show acetic acid-induced intestinal ulcers in a 1-day injury + vehicle rat (**A**), a 4-day injury + vehicle rat (**B**), and a 4-day injury + M64HCl rat (**C**). The black arrow indicates the ulcer area. Ulcer areas were quantified using ImageJ software. The ruler's smallest unit is 1 mm. Statistical analysis of the acetic acid-induced intestinal ulcer areas (**D**) shows a significant reduction in the 4-day injury + M64HCl treatment group compared to the 4-day injury + vehicle group. The scatter plot graphs display individual data points, means, and standard deviation (SD) error bars

granulocytes, and lymphocytes are recruited to the injury site and release chemokines and cytokines, triggering local inflammatory responses [22, 23]. Simultaneously, a wound-healing process is initiated with the aim of re-establishing the mucosal epithelial barrier and reinstating intestinal homeostasis, thereby resolving the inflammation. Depending upon the size and depth of the injury, the intestinal epithelial wound healing process may encompass restitution, proliferation, differentiation, and maturation [24, 25]. Restitution begins with epithelial cells migrating into the wound within hours. This is followed by the proliferation of epithelial cells over several hours to days, and ultimately differentiation of intestinal stem cells into all mature intestinal cell types [26]. Intestinal epithelial cells adjacent to wounds lose polarity, flatten, and adopt a migratory phenotype that facilitates the resurfacing of the injury [27]. The regulation of collective epithelial cell migration relies heavily on epithelial

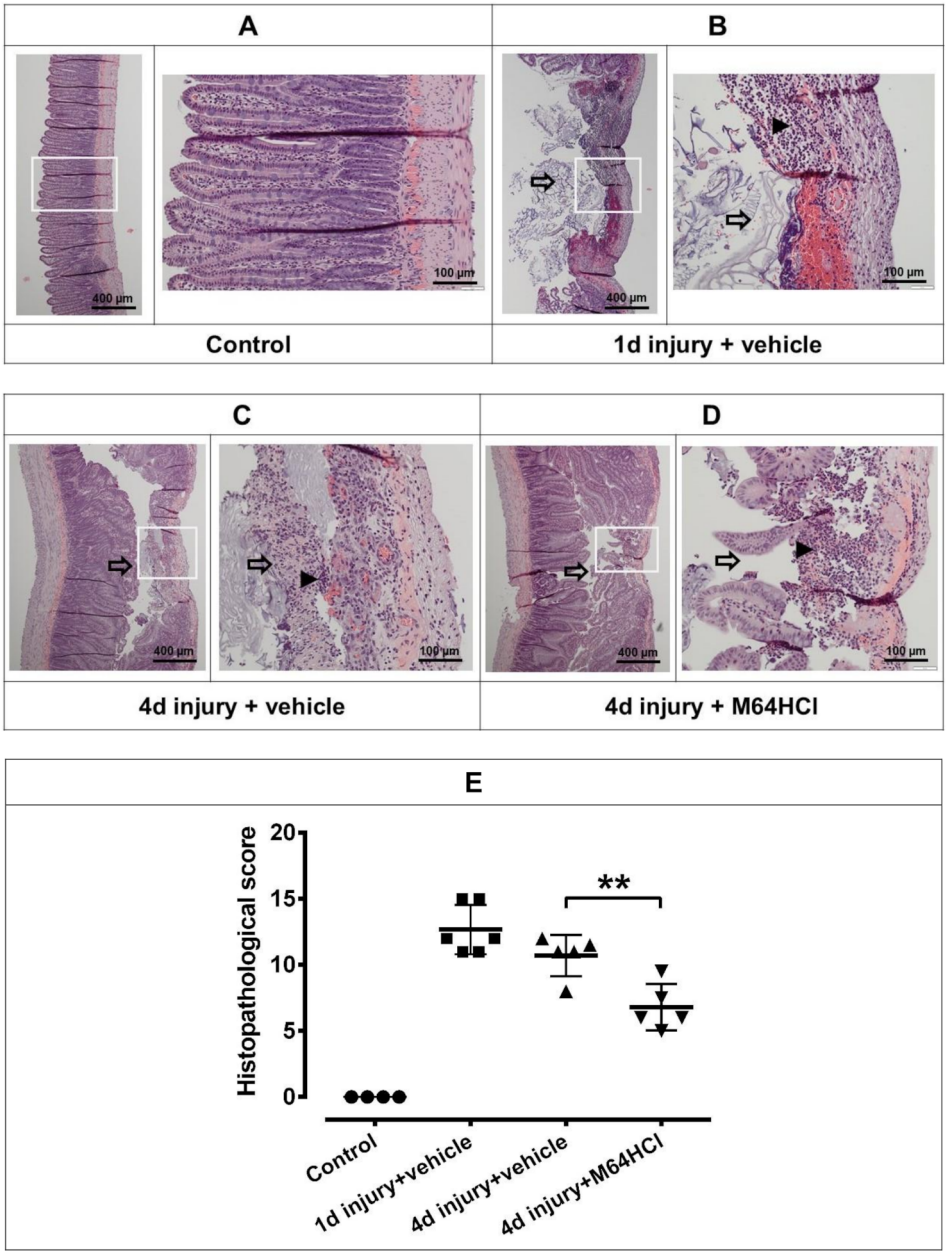

Fig. 2 Histopathology of intestinal tissue. Intestinal tissues including ulcerated areas were collected from the normal control (**A**), 1-day injury + vehicle (**B**), 4-day injury + vehicle (**C**), and 4-day injury + M64HCl (**D**) groups and stained with hematoxylin and eosin (H&E). The left panels show low-magnification (40x) images of ulcerated areas and adjacent tissues, while the right panels display the same sections at higher magnification (200x), focusing on the ulcerated areas. The white square indicates where the high-magnification image was taken. The black arrow indicates the ulcer area. The black arrowheads indicate infiltration of inflammatory cells. Histopathological analysis revealed better healing in the 4-day injury + M64HCl group compared to the 4-day injury + vehicle group (**E**). The scatter plot graphs show individual data points along with mean values and SD error bars

cell-cell junctions and adhesive interactions with the substrate [20]. Numerous molecular mechanisms and pathways coordinate epithelial cell migration. One important mechanism involves β1 integrin heterodimers, which regulate the formation of focal adhesions (FA) by facilitating the recruitment and autophosphorylation of the FA-associated proteins FAK and Src, subsequently activating paxillin and p130Cas [28, 29].

Previous studies have shown that FAK activation promotes cell migration across various types of cells. An early study revealed an increase in FAK activation in migrating keratinocytes during in vitro epidermal wound healing [30]. Inhibition of FAK with Y15 significantly reduced the migration ability of vascular endothelial cells [31]. Embryonic fibroblasts from FAK knockout mice exhibited severe migration defects [32]. Conversely,

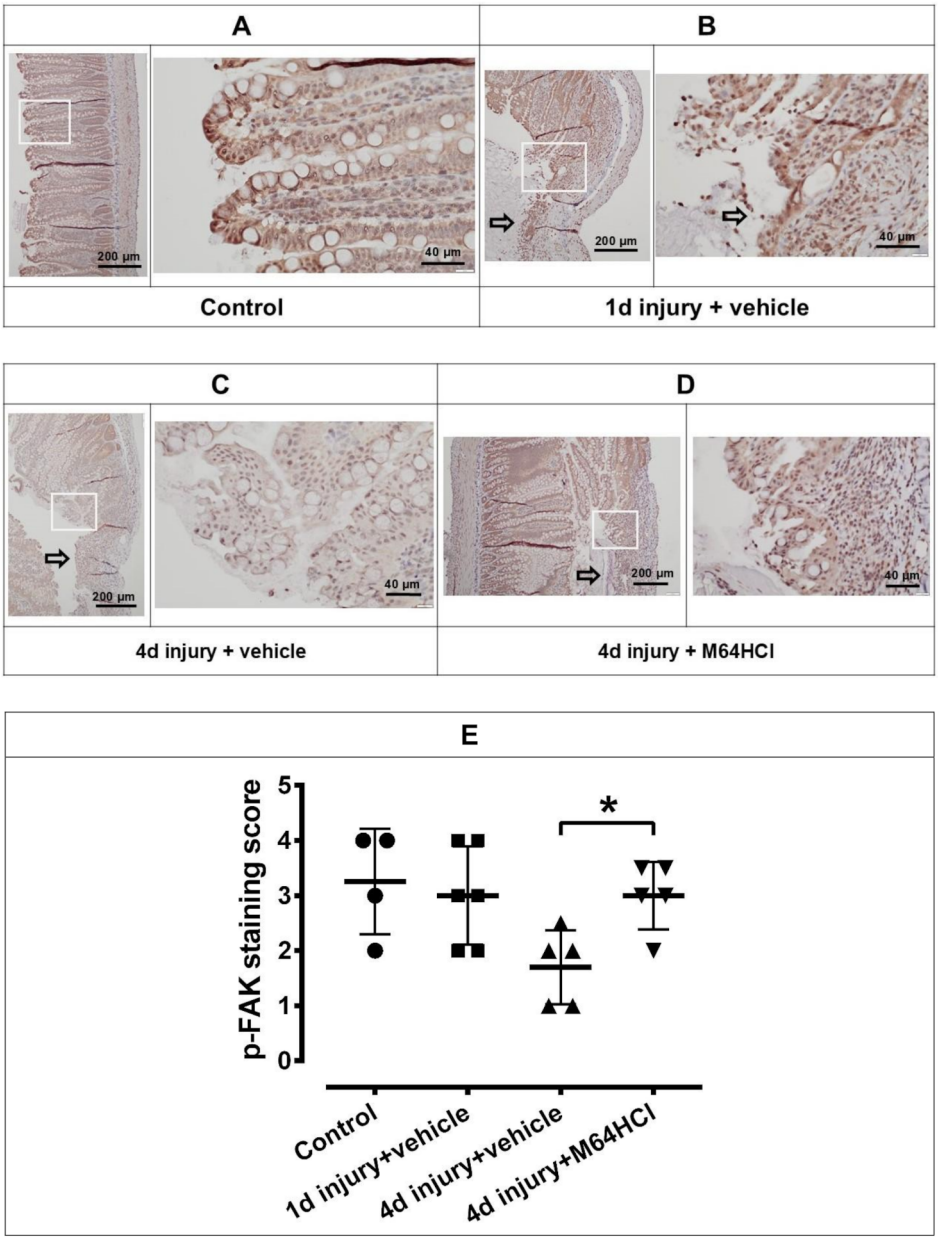

Fig. 3 Continuous sections used for H&E staining were also used to examine p-FAK expression through immunohistochemistry. This figure presents representative images of p-FAK immunohistochemical staining (brown) in the intestines of the normal control (**A**), 1-day injury + vehicle (**B**), 4-day injury + vehicle (**C**), and 4-day injury + M64HCl (**D**). p-FAK expression in the intestinal epithelial cells at the edge of the ulcer area is decreased in the 4-day injury + vehicle group, but returns to normal levels in the 4-day injury + M64HCl group (**E**). The left panels show low-magnification (40x) images, while the right panels display the same sections at higher magnification (200x). The white square indicates where the high-magnification image was taken. The black arrow indicates the ulcer area. The scatter plot graphs display individual data points, means, and SD error bars

overexpression of FAK in Chinese hamster ovary cells promotes their migration on fibronectin [33]. Our previous study indicated that the migration of Caco-2 intestinal epithelial cells is linked to increased FAK phosphorylation [34]. Recently, Su et al. discovered that heparin-binding EGF-like growth factor (HB-EGF) enhances the migration and adhesion of rat intestinal epithelial cells (RIE-1 cells) through focal adhesion kinase [35]. Additionally, l-arginine promotes the migration of IPEC-J2 cells, derived from the jejunum of newborn piglets, via a FAK-dependent mechanism [36]. However, activated FAK is reduced at the edges of intestinal epithelial monolayer wounds in vitro [9] and around human gastric and colonic ulcers in vivo [10]. Multiple factors may contribute to the reduced p-FAK levels at the wound edge, [37, 38] including: (1) Disruption of cell-cell adhesion: As

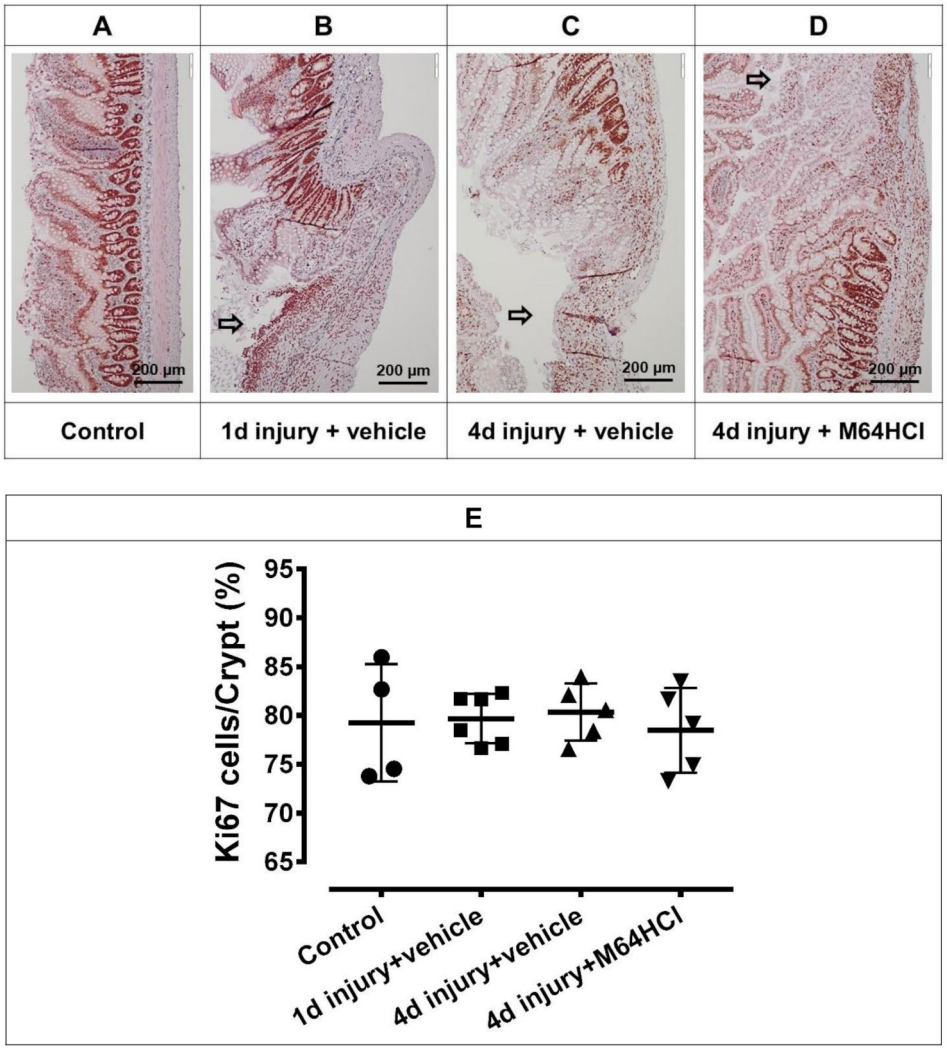

Fig. 4 Immunohistochemistry staining of Ki67 ($n = 4–6$). Representative images of Ki67 immunohistochemistry staining (brown color) in the intestines of the normal control (**A**), 1-day injury + vehicle (**B**), 4-day injury + vehicle (**C**) or 4-day injury + M64HCl (**D**) are shown in this figure. There was no significant difference in the percentage of Ki67-positive cells in each crypt at the edge of the ulcer area among all groups (**E**). The black arrow indicates the ulcer area. The scatter plot graphs show individual data points along with mean values and SD error bars

Table 1 Serum ALT, AST, and creatinine levels (mean ± SD) were compared between the 4-day injury + vehicle group and the 4-day injury + M64HCl group

	4d injury + vehicle	4d injury + M64HCl	*P*-value
Serum ALT (U/L)	90.89 ± 5.71	100.36 ± 23.44	0.41
Serum AST (U/L)	29.19 ± 4.27	32.29 ± 4.40	0.29
Serum Creatinine (μg/ml)	2.57 ± 1.00	3.17 ± 0.49	0.27

epithelial cells migrate away from adjacent cells toward the injury site, intercellular connections may be disrupted, leading to decreased FAK signaling. (2) Modified cell-matrix interactions: Migrating cells engage with the extracellular matrix in a manner that may differ from interactions in intact epithelium, potentially influencing FAK activity. (3) Cytoskeletal remodeling: Changes in the cytoskeleton - an essential component for cell motility - may occur at the wound edge, thereby altering FAK signaling pathways.

These studies led us to explore whether activating FAK can enhance epithelial restitution and accelerate intestinal mucosa healing. We recently synthesized a new FAK activator, M64HCl, that shows promising drug-like properties [13]. With a molecular weight of less than 500, solubility greater than 100 μM, and a log D value between 0 and 3, it has a high likelihood of good

intestinal permeability. Our previous research showed that M64HCl activates FAK-Tyr397 in Caco-2 cells in a dose-dependent manner, with p-FAK-Tyr397 increasing by 8.7 ± 3.0%, 9.1 ± 3.9%, 20.2 ± 7.4%, 25.3 ± 7.8%, and 28.4 ± 9.3% at concentrations of 100 pM, 1, 10, 100, and 1000 nM, respectively. Continuous infusion of M64HCl at 25 mg/kg/day promoted the healing of ischemic jejunal ulcers and indomethacin-induced small intestinal injury in C57Bl/6 mice [13]. The current study using a rat model further demonstrated that administering M64HCl increased p-FAK expression in intestinal epithelial cells in this second species, as evidenced by immunohistochemical staining, and accelerated the healing of acetic acid-induced ischemic ulcers. This was shown by a reduced ulcer area and improved histological changes compared to the 4-day injury + vehicle group. Interestingly, we found there was no significant difference in the percentage of Ki67-positive cells in each crypt at the edge of the ulcer area among all groups, suggesting that this small molecule promotes mucosal healing by increasing migration rather than by stimulating proliferation. Additionally, we stained for cleaved caspase-3 as an apoptosis marker. Upon reviewing the staining, we observed some positively stained cells in the villi but very few in the ulcer and its adjacent areas across all groups (data not shown). Therefore, we do not believe apoptosis plays a role in the epithelial repair promoted by M64HCl.

FAK promotes cell migration by activating multiple signaling pathways that involve kinases and the phosphorylation of other FA components. When integrins bind to the extracellular matrix (ECM), they induce a conformational change to allow for FAK autophosphorylation at Y397, creating binding sites for Src family kinases. The binding of Src to these sites further phosphorylates additional residues on FAK (pY576 or pY577), resulting in the formation and full activation of the FAK–Src complex [39]. The activated FAK–Src complex can then phosphorylate p130Cas (Crk-associated substrate, also known as BCAR1). Phosphorylated p130Cas interacts with adaptors Crk, Crk-L, CRKII, and Nck, assembling p130Cas-Crk-dedicator of cytokinesis 1 (DOCK180) complex, [40] which recruits the small GTPase RAC1 to the membrane. This recruitment induces actin cytoskeleton remodeling, pseudopodia extension and focal adhesion turnover, ultimately increasing cell migration [41]. In addition, the FAK/Src kinase complex can activate paxillin at Try31 and Tyr118 [42]. Activated paxillin recruits the PKL-PIX-PAK-Nck complex to the focal adhesion, regulating the actin dynamics, and promoting cell spreading and migration through Rac and Cdc42 [43, 44, 45]. Recent work from our laboratory has demonstrated the activation of some of these signaling elements in cultured intestinal epithelial cell lines after treatment with our original prototype molecule ZINC40099027 or with M64HCl [46].

In addition, the serum concentration of M64HCl reached 726.8 ± 461.3 nM during continuous infusion at a dosage of 25 mg/kg/day in the current study. Notably, this dosage did not affect liver or kidney function, as evidenced by serum levels of ALT, AST, and creatinine comparable to those in the injury + vehicle group. In fact, our previous cytotoxicity assay demonstrated that M64HCl exhibits cytotoxicity at 1 mM in IMR-90 human pulmonary fibroblasts and at 200 μM in SH-SY5Y human neuronal cells—concentrations much higher than the current serum levels of M64HCl [13]. Furthermore, our previous study [13]. also showed that M64HCl accumulates in the kidneys and gastrointestinal mucosa, and functional nephrectomy studies suggest that it is predominantly excreted in the urine, indicating that it is not metabolized in the body.

One limitation of this study is the lack of measurement of systemic inflammatory markers, such as IL-1β and TNF-α, as well as intestinal barrier permeability, which could provide additional insights into the effectiveness of M64HCl in promoting intestinal mucosal healing. In addition, since the effect of FAK activation on the immune system was not the focus of this study, we did not further characterize the different types of inflammatory leukocytes here. However, this represents an interesting subject for future investigation beyond the scope of the present study. In conclusion, this study using a rat model further supports that M64HCl, a novel FAK activator, enhances intestinal mucosal healing without significant toxicity. Further investigation in other gastrointestinal injury models is required to validate these findings. Additionally, the potential mechanism of action of M64HCl through the FAK-Src complex will be explored in vivo in future research.

Abbreviations

ALT	Alanine aminotransferase
AST	Aspartate aminotransferase
DMSO	Dimethyl sulfoxide
FA	Focal adhesions
FAK	Focal adhesion kinase
GI	Gastrointestinal
PPIs	Proton pump inhibitors
NSAIDs	Nonsteroidal anti-inflammatory drugs
UPLC-MS	Ultra-performance liquid chromatography-mass spectrometry
ZINC	ZINC is not commercial

Acknowledgements

The immunohistochemistry staining was performed in the Tissue Resources Core Shared Resource at the Case Comprehensive Cancer Center (P30 CA043703).

Author contributions

GL and MB designed the experiment. GL, AE, and LK conducted the animal experiments and analyzed the data. RGM and VG provided the compound. GL drafted the manuscript. MB and VG obtained funding. All authors carefully read, edited, and approved the final manuscript.

Funding
This study was supported by a subaward (C00066571-14) of grant U01HL152410 from the National Institutes of Health (NIH). This research was partially supported by the National Institutes of Health's National Center for Advancing Translational Sciences, grant UL1TR002494.

Data availability
The raw data for the preparation of this article are available from the corresponding author upon reasonable request.

Declarations

Ethics approval and consent to participate
All experimental procedures involving animals were approved by the Institutional Animal Care and Use Committee (IACUC) of Northeast Ohio Medical University, with IACUC number 23-04-366. The experiments were conducted in accordance with relevant guidelines and regulations.

Consent for publication
Not applicable.

Competing interests
The University of North Dakota and the University of Minnesota have filed two patent applications on the use of small-molecule FAK activators to promote mucosal healing. MDB and VJG are listed as co-inventors, and one also includes RGM.

Received: 29 July 2024 / Accepted: 24 April 2025
Published online: 08 May 2025

References

1. Hu X, Yuan X, Zhang G, et al. The intestinal epithelial-macrophage-crypt stem cell axis plays a crucial role in regulating and maintaining intestinal homeostasis. Life Sci. 2024;344:122452.
2. Tai FWD, McAlindon ME. NSAIDs and the small bowel. Curr Opin Gastroenterol. 2018;34(3):175–82.
3. Goddard AF, James MW, McIntyre AS, Scott BB. Guidelines for the management of iron deficiency anaemia. Gut. 2011;60(10):1309–16.
4. Lee HS, Nam JH, Oh DJ, Moon YR, Lim YJ. Reduced risk of Gastrointestinal bleeding associated with eupatilin in aspirin plus acid suppressant users: nationwide population-based study. Korean J Intern Med. 2024;39(2):261–71.
5. Tian L, Huang C, Fu W, et al. Proton pump inhibitors May enhance the risk of digestive diseases by regulating intestinal microbiota. Front Pharmacol. 2023;14:1217306.
6. Guidetti GF, Torti M, Canobbio I. Focal adhesion kinases in platelet function and thrombosis. Arterioscler Thromb Vasc Biol. 2019;39(5):857–68.
7. Kleinschmidt EG, Schlaepfer DD. Focal adhesion kinase signaling in unexpected places. Curr Opin Cell Biol. 2017;45:24–30.
8. Owen KA, Abshire MY, Tilghman RW, Casanova JE, Bouton AH. FAK regulates intestinal epithelial cell survival and proliferation during mucosal wound healing. PLoS ONE. 2011;6(8):e23123.
9. Basson MD, Sanders MA, Gomez R, et al. Focal adhesion kinase protein levels in gut epithelial motility. Am J Physiol Gastrointest Liver Physiol. 2006;291(3):G491–499.
10. Walsh MF, Ampasala DR, Hatfield J, et al. Transforming growth factor-beta stimulates intestinal epithelial focal adhesion kinase synthesis via Smad- and p38-dependent mechanisms. Am J Pathol. 2008;173(2):385–99.
11. Yu CF, Sanders MA, Basson MD. Human caco-2 motility redistributes FAK and paxillin and activates p38 MAPK in a matrix-dependent manner. Am J Physiol Gastrointest Liver Physiol. 2000;278(6):G952–966.
12. Wang Q, More SK, Vomhof-DeKrey EE, Golovko MY, Basson MD. Small molecule FAK activator promotes human intestinal epithelial monolayer wound closure and mouse ulcer healing. Sci Rep. 2019;9(1):14669.
13. Wang Q, Gallardo-Macias R, Vomhof-DeKrey EE, et al. A novel drug-like water-soluble small molecule focal adhesion kinase (FAK) activator promotes intestinal mucosal healing. Curr Res Pharmacol Drug Discov. 2023;4:100147.
14. Okabe S, Amagase K. An overview of acetic acid ulcer models–the history and state of the Art of peptic ulcer research. Biol Pharm Bull. 2005;28(8):1321–41.
15. Flanigan TL, Owen CR, Gayer C, Basson MD. Supraphysiologic extracellular pressure inhibits intestinal epithelial wound healing independently of luminal nutrient flow. Am J Surg. 2008;196(5):683–9.
16. Owen CR, Yuan L, Basson MD. Smad3 knockout mice exhibit impaired intestinal mucosal healing. Lab Invest. 2008;88(10):1101–9.
17. Kovalenko PL, Kunovska L, Chen J, Gallo KA, Basson MD. Loss of MLK3 signaling impedes ulcer healing by modulating MAPK signaling in mouse intestinal mucosa. Am J Physiol Gastrointest Liver Physiol. 2012;303(8):G951–960.
18. Kovalenko PL, Flanigan TL, Chaturvedi L, Basson MD. Influence of defunctionalization and mechanical forces on intestinal epithelial wound healing. Am J Physiol Gastrointest Liver Physiol. 2012;303(10):G1134–1143.
19. Zhou R, He L, Zhang J, et al. Molecular basis of TMPRSS2 recognition by paeniclostridium sordellii hemorrhagic toxin. Nat Commun. 2024;15(1):1976.
20. Boger KD, Sheridan AE, Ziegler AL, Blikslager AT. Mechanisms and modeling of wound repair in the intestinal epithelium. Tissue Barriers. 2023;11(2):2087454.
21. Iizuka M, Konno S. Wound healing of intestinal epithelial cells. World J Gastroenterol. 2011;17(17):2161–71.
22. Xue X, Falcon DM. The role of immune cells and cytokines in intestinal wound healing. Int J Mol Sci. 2019;20(23):6097.
23. Leoni G, Neumann PA, Sumagin R, Denning TL, Nusrat A. Wound repair: role of immune-epithelial interactions. Mucosal Immunol. 2015;8(5):959–68.
24. Sommer K, Wiendl M, Müller TM, et al. Intestinal mucosal wound healing and barrier integrity in IBD-Crosstalk and trafficking of cellular players. Front Med (Lausanne). 2021;8:643973.
25. Oncel S, Basson MD. Gut homeostasis, injury, and healing: new therapeutic targets. World J Gastroenterol. 2022;28(17):1725–50.
26. Otte ML, Lama Tamang R, Papapanagiotou J, Ahmad R, Dhawan P, Singh AB. Mucosal healing and inflammatory bowel disease: therapeutic implications and new targets. World J Gastroenterol. 2023;29(7):1157–72.
27. Basson MD, Rashid Z, Turowski GA, et al. Restitution at the cellular level: regulation of the migrating phenotype. Yale J Biol Med. 1996;69(2):119–29.
28. Huttenlocher A, Horwitz AR. Integrins in cell migration. Cold Spring Harb Perspect Biol. 2011;3(9):a005074.
29. Zhao X, Guan JL. Focal adhesion kinase and its signaling pathways in cell migration and angiogenesis. Adv Drug Deliv Rev. 2011;63(8):610–5.
30. Gates RE, King LE Jr., Hanks SK, Nanney LB. Potential role for focal adhesion kinase in migrating and proliferating keratinocytes near epidermal wounds and in culture. Cell Growth Differ. 1994;5(8):891–9.
31. Yu H, Gao M, Ma Y, Wang L, Shen Y, Liu X. Inhibition of cell migration by focal adhesion kinase: Time-dependent difference in integrin-induced signaling between endothelial and hepatoblastoma cells. Int J Mol Med. 2018;41(5):2573–88.
32. Ilić D, Furuta Y, Kanazawa S, et al. Reduced cell motility and enhanced focal adhesion contact formation in cells from FAK-deficient mice. Nature. 1995;377(6549):539–44.
33. Cary LA, Chang JF, Guan JL. Stimulation of cell migration by overexpression of focal adhesion kinase and its association with Src and Fyn. J Cell Sci. 1996;109(Pt 7):1787–94.
34. Liu YW, Sanders MA, Basson MD. Human Caco-2 intestinal epithelial motility is associated with tyrosine kinase and cytoskeletal focal adhesion kinase signals. J Surg Res. 1998;77(2):112–8.
35. Su Y, Besner GE. Heparin-binding EGF-like growth factor (HB-EGF) promotes cell migration and adhesion via focal adhesion kinase. J Surg Res. 2014;189(2):222–31.
36. Rhoads JM, Chen W, Gookin J, et al. Arginine stimulates intestinal cell migration through a focal adhesion kinase dependent mechanism. Gut. 2004;53(4):514–22.
37. Tilghman RW, Slack-Davis JK, Sergina N, et al. Focal adhesion kinase is required for the Spatial organization of the leading edge in migrating cells. J Cell Sci. 2005;118(Pt 12):2613–23.
38. Jiang X, Jacamo R, Zhukova E, Sinnett-Smith J, Rozengurt E. RNA interference reveals a differential role of FAK and Pyk2 in cell migration, leading edge formation and increase in focal adhesions induced by LPA in intestinal epithelial cells. J Cell Physiol. 2006;207(3):816–28.
39. Katoh K. FAK-Dependent cell motility and cell elongation. Cells. 2020;9(1):192.
40. Schlaepfer DD, Broome MA, Hunter T. Fibronectin-stimulated signaling from a focal adhesion kinase-c-Src complex: involvement of the Grb2, p130cas, and Nck adaptor proteins. Mol Cell Biol. 1997;17(3):1702–13.
41. Cabodi S, del Pilar Camacho-Leal M, Di Stefano P, Defilippi P. Integrin signalling adaptors: not only figurants in the cancer story. Nat Rev Cancer. 2010;10(12):858–70.

42. Pasapera AM, Schneider IC, Rericha E, Schlaepfer DD, Waterman CM. Myosin II activity regulates vinculin recruitment to focal adhesions through FAK-mediated paxillin phosphorylation. J Cell Biol. 2010;188(6):877–90.
43. Parsons JT, Horwitz AR, Schwartz MA. Cell adhesion: integrating cytoskeletal dynamics and cellular tension. Nat Rev Mol Cell Biol. 2010;11(9):633–43.
44. Turner CE. Paxillin interactions. J Cell Sci. 2000;113:4139–40.
45. Miller AE, Hu P, Barker TH. Feeling things out: bidirectional signaling of the cell-ECM interface, implications in the mechanobiology of cell spreading, migration, proliferation, and differentiation. Adv Healthc Mater. 2020;9(8):e1901445.
46. Oncel S, Basson MD. ZINC40099027 promotes monolayer circular defect closure by a novel pathway involving cytosolic activation of focal adhesion kinase and downstream paxillin and ERK1/2. Cell Tissue Res. 2022;390(2):261–79.

Publisher's note